

Connecting Shear Stress Relaxation and Enthalpy Recovery in Polymers through a Modified TNM Approach

L. Andreozzi,* M. Faetti, F. Zulli, and M. Giordano

Dipartimento di Fisica "E. Fermi" and INFM, Università di Pisa, via F. Buonarroti 2, 56127 Pisa, Italy

Received April 5, 2004; Revised Manuscript Received June 29, 2004

ABSTRACT: The Tool–Narayanaswamy–Moynihan model (TNM) is widely accepted in order to describe the enthalpy recovery mechanism of polymers. However, some problems have been found in quantitative analysis as far as the parameters of the model are concerned. In particular, in several studies, the values of the Kauzmann temperature have been obtained 150 K or more below the glass transition, whereas other works have provided values of the activation energy of the relaxation times at the glass transition that are inconsistent with viscoelastic or dielectric measurements. In this paper, we analyze differential scanning calorimetry experiments in a low molecular weight PMMA sample in terms of a modified TNM model, where the adjustable parameters only provide the behavior of the out-of-equilibrium relaxation times. The temperature dependence of the equilibrium relaxation times is instead set at the values determined by the shear viscosity data of the sample. A good agreement between theory and experiments is obtained suggesting that the difficulties quoted above could actually depend on the TNM handling of the nonlinear effects.

I. Introduction

One of the distinctive features of glass-forming systems is the dramatic slowing down of molecular mobility when the glass transition is approached, while, at the same time, changes in the structural properties are not observed.¹ For this reason, the structural relaxation of these materials is intensively studied by means of many different experimental techniques.² In particular, differential scanning calorimetry (DSC) experiments are performed in order to investigate the enthalpy relaxation (or better enthalpy recovery) mechanism of glasses. An interesting question concerns the comparison of the temperature dependence of the relaxation times of the different observables. In several studies it was found that the apparent activation energy at the glass transition coincided for enthalpy relaxation and viscous flow³ or dielectric relaxation. This finding has been recently validated by works in which the fragility of glass-forming systems, as evaluated by thermal methods, was compared with the fragility obtained by viscoelastic or dielectric measurements.^{4,5}

The parameters describing the enthalpy relaxation of glass-formers can be also obtained by analyzing the DSC experiments in the framework of phenomenological approaches such as the Tool–Narayanaswamy–Moynihan or the Scherer–Hodge models.

These approaches are able to reproduce the main features of the structural relaxation process. However, when the material parameters are obtained by optimizing the agreement between the experimental DSC curves and the predictions of the models, some inconsistencies are often found. In particular, values of the Kauzmann temperature lower than the glass transition temperature T_g by 150 K or more have been obtained in several studies,^{6–9} whereas in other cases the activation energy at T_g resulted inconsistent with the cooling rate dependence of T_g or with the viscoelastic or dielectric fragility.¹⁰ Of these flaws, the former has been

recently addressed by Hutchinson and co-workers⁹ that modified the Scherer–Hodge handling of nonlinearity, to provide higher values of the Kauzmann temperature. However an additional free parameter was introduced in their model. In our opinion too, the difficulties above outlined could be related to the way in which these approaches handle the nonlinearity of the structural relaxation with the assumption of a specific structure dependence of the instantaneous relaxation times. In this paper is proposed a simple modification of the TNM model where the fitting parameters provide only the behavior of the out of equilibrium relaxation times, while the temperature dependence of the equilibrium relaxation times can be treated independently.

II. Theoretical Background

To start with, we report the basic assumptions and relations of the TNM model. Its constitutive equation can be obtained in terms of the evolution of the fictive temperature T_f first introduced by Tool to describe the structural state of a glass.¹¹ This parameter represents the relaxational part of the enthalpy and is implicitly defined by the following relation:¹²

$$H(T) = H_{eq}(T_f) - \int_{T_f}^{T_i} C_p^{glass}(\theta) d\theta \quad (1)$$

$H_{eq}(T_f)$ is the equilibrium value of the enthalpy H at the temperature T_f , and $C_p^{glass}(T)$ is the unrelaxed glassy heat capacity. By differentiating eq 1 one obtains

$$\frac{dT_f}{dT} = \frac{(C_p(T) - C_p^{glass}(T))}{\Delta C_p(T_f)} \approx \frac{(C_p(T) - C_p^{glass}(T))}{\Delta C_p(T)} \equiv C_p^N(T) \quad (2)$$

where $\Delta C_p(T) = C_p^{liq}(T) - C_p^{glass}(T)$ is the heat capacity increment between the glassy and liquid state. All the quantities in the right side of eq 2 can be experimentally measured by means of a DSC apparatus, so that several

* Corresponding author. E-mail laura.andreozzi@df.unipi.it.

normalized heat capacity curves $C_p^N(T)$ can be obtained following different thermal histories. In fact,¹² the DSC traces recorded after cooling and annealing in the glass show an overshooting peak whose shape and position are strongly dependent on the thermal history. These scans are then compared with the theoretical predictions obtained by numerically solving the basic equation of the TNM model:¹²

$$T_f(T) = T_0 + \int_{T_0}^T dT' \left\{ 1 - \exp\left(-\left[\int_{T'}^T \frac{dT''}{Q\tau(T_f, T'')}\right]^\beta\right) \right\} \quad (3)$$

T_0 is a reference temperature well above the glass transition temperature, $Q = Q_{c,h}$ represents the cooling/heating rate, while β is the nonexponentiality parameter determining the broadness of the relaxation spectrum. If an annealing procedure is performed at a temperature T_a for a time t_a , the term

$$\int_0^{t_a} \frac{dt'}{\tau(T_f(t'), T_a)}$$

has to be added to the reduced time calculus in the second integration of eq 3. The model is completed by assuming a specific expression for the temperature and structure dependence of the relaxation time $\tau(T, T_f)$. The most widely used are the Narayanaswamy–Moynihan (NM)^{13,14} and the Scherer–Hodge (SH)^{8,15} ones:

$$\tau(T_f, T) = A \exp\left\{\frac{x\Delta h}{RT} + \frac{(1-x)\Delta h}{RT_f}\right\} \quad \text{NM} \quad (4)$$

$$\tau(T_f, T) = A \exp\left\{\frac{B}{RT(1 - T_2/T_f)}\right\} \quad \text{SH} \quad (5)$$

When the NM expression is employed, this formalism is usually referred to as TNM model, whereas, when the SH expression is assumed, the approach is usually called AGV (Adam–Gibbs–Vogel) model. The SH expression appears to be more reliable than the NM one because it can be developed in the framework of the Adam–Gibbs theory¹⁶ and because at equilibrium ($T_f = T$) the Vogel–Fulcher–Tamman law^{17–19} is recovered. However, it has been shown that these expressions are quite similar regarding the predictive power of the model.^{6,12} A key feature of the TNM or AGV approach is that the same parameters provide both the equilibrium temperature dependence and the out-of-equilibrium structure dependence of the relaxation time. So, if the parameters are obtained by fitting experimental DSC traces, whose shape is mainly related to the behavior of the system in the out-of-equilibrium state, it is possible that some inconsistencies are found concerning the equilibrium behavior if the relation assumed for $\tau(T, T_f)$ is not suitably correct.

To gain further insight, it would be useful to separate the equilibrium temperature dependence of the relaxation time from its out-of-equilibrium behavior. To this aim, we followed the general procedure employed by Avramov and Gutzov in developing their relaxation model²⁰ by setting

$$\tau = A \cdot \exp\left[\frac{E(T, z)}{RT}\right] \quad (6)$$

In eq 6 the activation energy E depends on the temper-

ature because of the non-Arrhenius character of the structural relaxation of glass-formers. The parameter $z = (T_f - T)/T$ represents a measure of the departure from equilibrium so that the dependence of E on z describes the nonlinear features of the structural relaxation. As soon as z is a small quantity, the activation energy can be expanded in a Taylor series (around $z = 0$) truncated to the linear term:

$$E(T, z) \approx E(T, 0) + \left(\frac{\partial E(T, z)}{\partial z}\right)_{z=0} \cdot z \quad (7)$$

From eq 6, one finally obtains

$$\tau = \tau^{\text{eq}}(T) \cdot \exp[-bz] \quad (8)$$

where b stands for

$$b = -\frac{1}{RT} \left(\frac{\partial E(T)}{\partial z}\right)_{z=0} \quad (9)$$

In this way one can assume for $\tau^{\text{eq}}(T)$ the same temperature dependence of the viscosity or the dielectric relaxation times and try to adjust the other parameters to fit the experimental DSC data. An apparently similar approach was recently proposed by Tverjanovich,²¹ which modified the TNM expression by assuming temperature dependence for the parameter Δh of eq 4. In his work, the viscosity data of Selenium (Se) were fitted by using the equation $\eta = \eta_0 \exp[E_\eta(T)]$ and then it was assumed $\Delta h = E_\eta(T)$. With this position, the temperature dependence of thermal expansion coefficient of Se at the glass transition was well reproduced by the TNM model, and it provided a value for the prefactor A in eq 4 of the order of the time of the atomic vibrations. Even if also the assumption $\Delta h = E_\eta(T)$ leads to relaxation times at equilibrium with the same temperature dependence of viscosity, our modification of TNM model seems to be more general because any empirical specific expression is not assumed. On the other hand, eq 8 is based on a first-order approximation so that this approach is expected to work only if the system is not too far from thermodynamic equilibrium.

Unfortunately, b in eq 9 could be a function of temperature and some additional hypotheses should be introduced. However in this work we want to adopt the same number of free parameters as in the standard TNM or AGV model. One of them is the prefactor in the relation chosen for the equilibrium relaxation time that is $\tau^{\text{eq}}(T) = A \cdot \eta$, a second one is the stretching factor β in eq 3 so that two parameters are left to provide the function $b(T)$. For some different choices of $b(T)$, we performed fitting procedures of DSC experiments carried out on a low molecular weight PMMA sample where we also performed viscoelastic measurements. In particular, b trial functions were adopted with linear ($b(T) = a + qT$) and different inverse ($b(T) = a + q/T$, $b(T) = a + q/T^2$, $b(T) = a/(q - T)$) T -dependencies. Results almost independent of the specific function assumed for $b(T)$ were obtained. This could be understood on the following basis: the values of temperature relevant to the structural relaxation at the glass transition can be taken into account in a restricted interval around it. In such a T range and with a and q values suited to a good C_p^N -curves fitting, the above b trial functions provided for $\partial E(T)/\partial z$ (see eq 9) increasing T -dependencies, differing from each other by few percent only. An example is given in Figure 1 where $\partial E(T)/\partial z|_{z=0}$ is plotted in a T range of 50 K around T_g for linear direct and inverse T

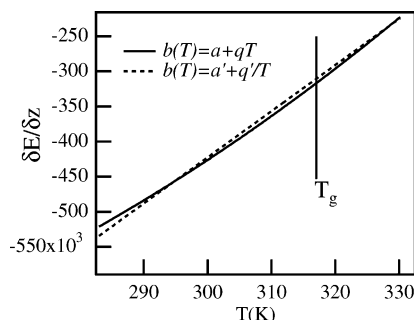


Figure 1. Temperature dependence around T_g of the PMMA sample of this work of $\partial E(T)/\partial z$ (eq 9) as obtained from the fitting of DSC experiments (see the Results and Discussion) for $b(T)$ with linear direct (continuous line) and inverse (dotted line) T dependence. The $\tau^{\text{eq}}-T$ dependence is assumed to follow the VFT parametrization of experimental sample viscosity.

dependence of $b(T)$ and assuming for $\tau^{\text{eq}}(T)$ a T dependence according to the Vogel–Fulcher–Tamman law followed by PMMA viscosity (see results and discussion section). Being our results a very weak function of the $b(T)$ setting, in this work we report and discuss only the analysis carried out for the linear direct $b(T)$ setting which provided the least deviations from DSC experiments.

III. Experimental Procedure

The PMMA sample was purchased from Labservice Analytica and used as received without any further purification. The sample was almost monodisperse with $M_w = 1460$ g/mol and $M_w/M_n = 1.07$. The glass transition temperature, measured according to the enthalpic definition²² for a cooling rate of 40 K/min, was $T_g = 317.3$ K.

A Perkin-Elmer DSC 7 apparatus, frequently calibrated with indium and zinc standards, was used for the calorimetric experiments. Highly pure nitrogen was used as a purge gas. For the annealing experiments the sample was first maintained at high temperature ($T_g + 50$ K) for some minutes, then it was cooled (at a rate $Q_c = 40$ K/min) to the selected aging temperature T_a where it was annealed for a time t_a and finally it was cooled again to the starting scan temperature T_s and reheated at 10 K/min, recording the signal. A reference scan (cooling at 40 K/min and heating at 10 K/min) was immediately recorded after the annealing measurements in order to evaluate the enthalpy lost on aging the sample (see the procedure described in the following section). Some simple cooling/heating experiments were also performed with different fixed values of the cooling rate.

The viscoelastic properties were measured with a stress controlled Haake RheoStress RS150H rheometer. The measurements were carried out in the linear response regime by undergoing the sample to a torque with parallel-plate (20 mm diameter) sensor system. The loading gap between the sensor plates was 0.750 mm at 373 K. The gap was chosen significantly larger than the sample chain length to ensure gap independent measurements. Thermal dilatation effects were taken into account by the rheometer varying automatically the parallel-plate gap.

The temperature control system consists of the HaakeTC501 accessory, equipped with two platinum thermoresistances (PT100) and with a thermal bath with circulation of refrigerant. The temperature at the sample was stable within 0.1 K during all measurements, which were carried out under highly pure nitrogen flow.

The zero shear viscosity was obtained from flow and creep experiments at different temperatures, and dynamic tests in the range 10^{-2} to 24.4 Hz, which provided independent evaluation of the viscosity.

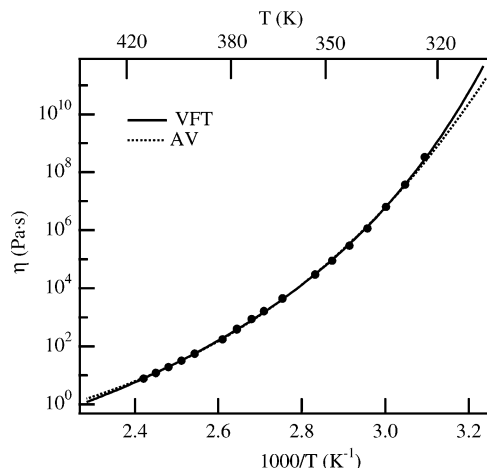


Figure 2. Temperature dependence of the shear viscosity in the PMMA sample (filled circles). The lines are the best fit obtained with the VFT law (continuous) and the Avramov expression, respectively. Best fit parameters are reported in the text.

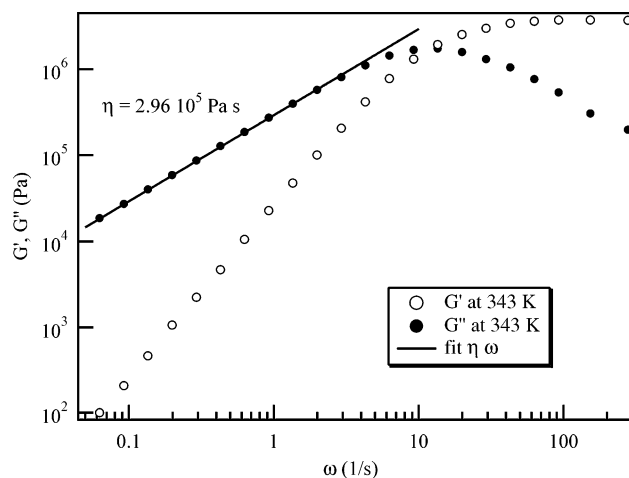


Figure 3. Example (at 343 K) of the calculation of zero shear viscosity from the loss modulus G'' according to $\eta = \lim_{\omega \rightarrow 0} G''/\omega$.²³

IV. Results and Discussion

In Figure 2, we report the temperature dependence of the PMMA viscosity, in the temperature range between 323 and 413 K.

At the highest temperatures down to 343 K, the viscosity was evaluated by both flow and creep experiments, below this temperature by creep and oscillatory data.²³ The dynamic experiments at 343 K are shown as an example in Figure 3. In Figure 2, the continuous line is the viscosity best fit obtained with the Vogel–Fulcher–Tamman law:

$$\eta(T) = \eta_0 \exp\left\{\frac{B}{R(T - T_0)}\right\} \quad (10)$$

with Vogel temperature $T_0 = 249 \pm 4$ K and pseudo-activation energy $B = 20.3 \pm 0.5$ kJ/mol. The dotted line is the best fit obtained according to the expression developed by Avramov²⁴ in his entropy-based model:

$$\eta(T) = \eta_0 \exp\left[30\left(\frac{T_r}{T}\right)^\alpha\right] \quad (11)$$

We obtained $T_r = 308 \pm 3$ K and $\alpha = 5.4 \pm 0.5$ for the

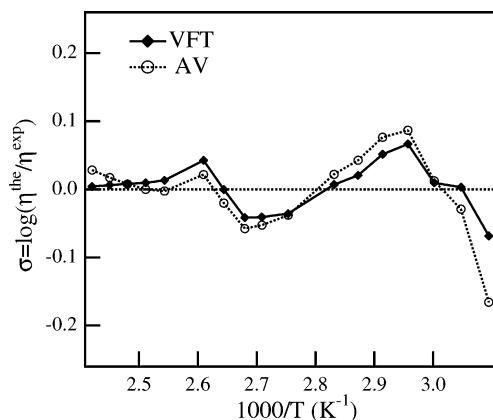


Figure 4. Logarithmic deviations ($\log(\eta^{\text{theor}}/\eta^{\text{expt}})$) from the experimental shear viscosity of the fits performed by means of the expressions of eqs 10 and 11.

best fit parameters. An inspection of the figure shows that the two equations fit the experimental data comparably. A more accurate analysis based on the logarithmic deviations $\sigma = \log(\eta^{\text{theor}}/\eta^{\text{expt}})$ indicates that the VFT law works slightly better in the description of the experimental data as shown in Figure 4. However the differences are very small so that it is difficult to single out the best from these expressions.

As far as the calorimetric experiments are concerned, we performed simultaneous fitting procedures aiming to reproduce six DSC traces recorded after different thermal histories. In fact, a key feature of the TNM or AGV models is that the adjustable parameters are material parameters and therefore they should be able to describe all the different experimental scans. The Nedler–Mead search routine²⁵ was employed to find the minimum of the average square deviation defined as

$$\sigma_a = \frac{1}{6N} \sum_{i=1}^6 \sum_{j=1}^N [w(i)\{C_{p,\text{expt}}^N(i,j) - C_{p,\text{theor}}^N(i,j)\}]^2 \quad (12)$$

In eq 12, the index i identifies the experimental scan whereas the index j denotes the points of each scan. To weight suitably the different DSC traces, the weighting factors $w(i)$ were assumed to be proportional to the inverse of the maximum of the overshooting peaks, with $w(i) = 1$ for the thermogram providing the highest peak. First, we analyzed our DSC experiments in the framework of the standard AGV model (see eq 5). Because of the well-known correlation among the model parameters,¹² several fitting procedures were carried out for different fixed T_2 values. The best set of parameters was then singled out by adopting a proper experimental strategy.²⁶ In Figure 5 we show the comparison between the experimental curves and their best fit obtained with the AGV model. The agreement between theory and experiments can be appreciated. However, even if the Adam–Gibbs temperature, $T_2 = 237 \pm 10$ K, was found to be compatible with the VFT temperature provided by the viscoelastic experiments, the evaluation from the best AGV parameters of the fragility, as measured by the steepness index:

$$m = \left. \frac{d[\log(\tau)]}{d(T_g/T)} \right|_{T_g} \quad (13)$$

was by about 25% higher than that obtained by the temperature dependence of viscosity.²⁶ To check if this

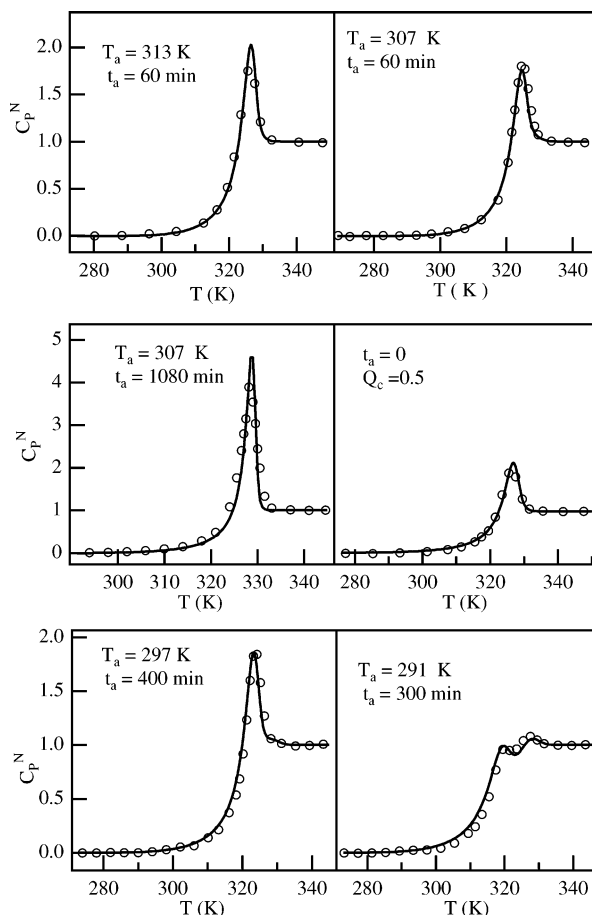


Figure 5. Results of the simultaneous fit (continuous line) by using the AGV model of six different experimental DSC traces of the PMMA sample (open circles). The best fit parameters are shown in Table 1.

discrepancy could be related to the relation assumed for $\tau(T, T_g)$, we fitted the DSC experiments by using the modified TNM approach of eqs 8 and 9. We assumed for $\tau^{\text{eq}}(T)$ the same temperature dependence as the viscosity, but with the two different parametrizations shown in Figure 2 (eqs 10 and 11). In fact, even if they provide very similar results for the viscosity, these parametrizations show a very different behavior below the glass transition, because only the VFT law provides a divergence of the relaxation times. So it could be possible to highlight differences by means of the calorimetric analysis. As a first step, we fitted two single curves recorded after having annealed the glass at two different temperatures. For each of them we assumed a constant value for the b parameter of eq 8. The two outcomes for b were then used in the simultaneous fitting as starting parameters for the linear temperature dependence assumed for $b(T)$. In Figures 6 and 7 the best fits obtained by using the VFT and the Avramov parametrization of the viscosity respectively are compared with the experimental DSC traces. The parameters found with the search routine are reported in Table 1 with the values of the average square deviation σ_a . The best fit parameters of the standard AGV model are also reported for comparison in the table. An inspection of Figures 5–7 shows that all the approaches are able to reproduce the experimental scans fairly well, even if eq 8 with the parametrization of eq 11 provides larger discrepancies in the experiments involving annealing at the two lowest temperatures. A more accurate

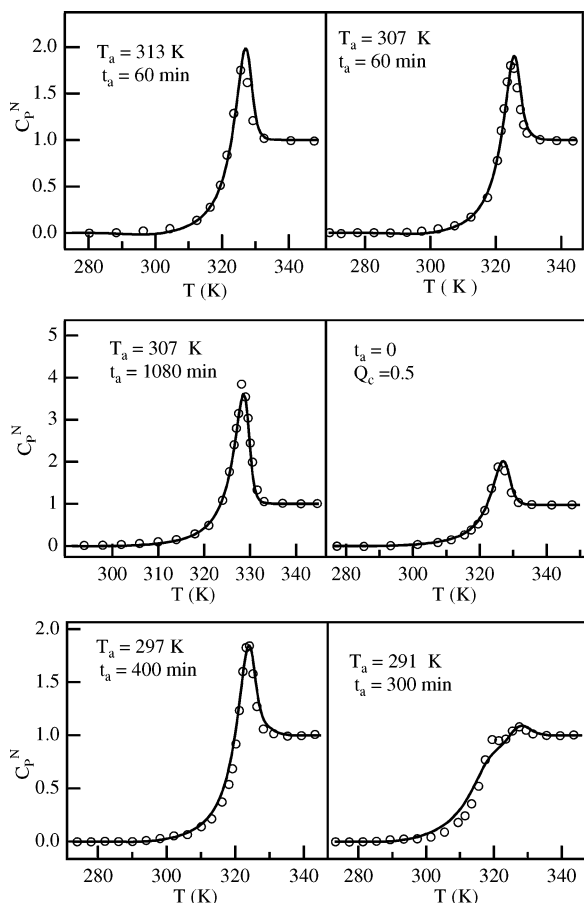


Figure 6. Best fit (continuous line) of the same DSC thermograms of Figure 5 obtained by adopting the modified TNM model described in the text, with the VFT parametrization of the equilibrium relaxation times (eq 10). The best fit parameters are reported in Table 1.

comparison through the analysis of the σ_a parameter confirms it, and this shows that the standard AGV model and eq 8 with VFT provide a better agreement than the Avramov parametrization. Between them, however, the modified approach with the VFT parametrization of the equilibrium relaxation times leads to a more reasonable value of the prefactor A than the one with AGV model. These results suggest that the inconsistencies often encountered in the equilibrium temperature dependence of the structural relaxation times as obtained by DSC experiments, could be actually ascribed to the expression assumed for $\tau(T, T_f)$ as also hypothesized in ref 9. To gain further insight, we analyzed the enthalpy relaxation isotherms. It is well-known that the area below the DSC traces recorded after having annealed the sample in the glass are related to the value of the enthalpy $\Delta H(T_a, t_a)$ lost during the annealing steps.^{12,27}

$$\Delta H(T_a, t_a) = \int_{T_x}^{T_y} \{C_p^a(T) - C_p^u(T)\} dT \quad (14)$$

where $C_p^a(T)$ is the heat capacity measured after annealing the sample at T_a for the time t_a , and $C_p^u(T)$ the heat capacity of the unannealed sample. T_x and T_y are reference temperatures ($T_x < T_g < T_y$). More precisely, the above expression provides the experimental enthalpy difference, at the starting scan temperature T_s , between the thermal treatments with and without the annealing. Such a value only represents an approxima-

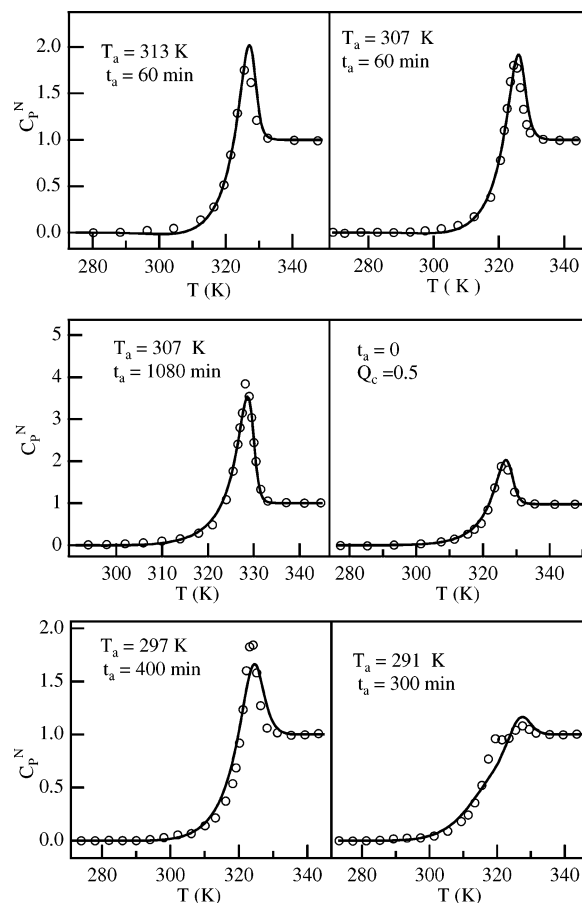


Figure 7. Best fit (continuous line) of the same DSC traces as in Figure 5 obtained by adopting the modified TNM model described in the text with the Avramov parametrization of the equilibrium relaxation times (eq 11). The best fit parameters are reported in Table 1.

Table 1. Best Fit Parameters Found by the Search Routine in the Fit of the Six DSC Experiments with the Standard AGV Model and the Modified Approach Described in the Text for the Two Different Parametrizations of $\tau^{\text{eq}}(T)$

parametrization	A (s)	B (kJ mol ⁻¹)	T_2 (K)	a	q	β	σ_a
Avramov	7.2×10^{-10}			329.2	-0.798	0.55	0.022
VFT	3.8×10^{-14}			1064	-2.977	0.46	0.015
AGV model	3.4×10^{-21}	35121	237			0.41	0.017

tion by defect of the enthalpy lost during the annealing^{26,28} and becomes very good only for low enough annealing temperatures. In the framework of TNM derived models, the experimental data obtained by means of eq 14 should be compared with the quantity²⁶

$$\Delta H(T_a, t_a)^{\text{theory}} = \Delta C_p(T_g) \cdot \{T_f^u(T_s) - T_f^a(T_s)\} \quad (15)$$

where the smooth temperature dependence of ΔC_p near the glass transition was neglected. In Figures 8 and 9 the experimental relaxation isotherms pertaining to two different annealing temperatures are compared with the theoretical predictions obtained with the modified TNM approach for the two different parametrizations of the equilibrium relaxation time. We can see that the results obtained by assuming the Avramov parametrization (eq 11) greatly overestimate the experimental data, whereas small deviations can be observed in the predictions of the VFT equation.

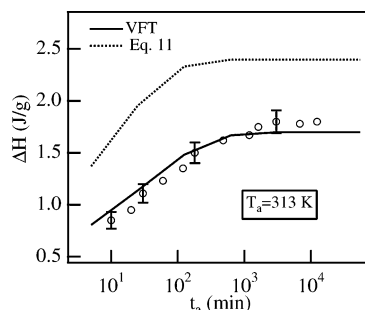


Figure 8. Enthalpy loss on aging the PMMA sample at $T_a = 313$ K for different aging times: experimental data (open circles) and the predictions of the modified TNM model for the two different parametrizations of the equilibrium relaxation times.

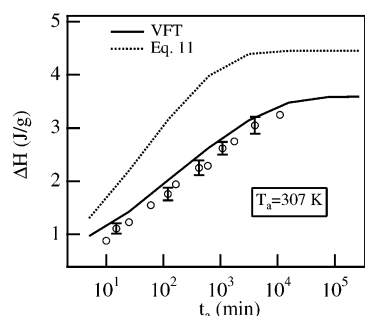


Figure 9. Enthalpy loss on aging the PMMA sample at $T_a = 307$ K for different times. The open circles are experimental data whereas the lines are the predictions of the modified TNM model for the two different parametrizations of the equilibrium relaxation times.

These results are mainly related to the different values of the glass transition temperature evaluated by those models. In fact, $T_f^u(T_g)$ in eq 15 is the glassy asymptotic value of the fictive temperature which represents the glass transition temperature according to the enthalpic definition. By analyzing the temperature dependence of the fictive temperature during a cooling at 40 K/min from the melt, we found $T_f^u(T_g) = 319.2$ K by assuming eq 11 and $T_f^u(T_g) = 317.0$ K in the case of VFT dependence. These values must be compared with the experimental $T_g = 317.3$ K.

So, both the analysis of the simultaneous fitting procedures and the enthalpy relaxation isotherms suggest that in the framework of this modified TNM approach, the VFT parametrization of the segmental relaxation dynamics is more appropriate than a smoother temperature dependence such as that provided by the Avramov expression.

This finding appears somewhat interesting and suitable to be compared with both theoretical²⁹ and experimental³⁰ works, in which it has been suggested that a kind of transition from the typical VFT-like behavior to an Arrhenius-type temperature dependence should be expected for the segmental dynamics on approaching the glass transition. Our results seems at variance with this possibility, even if it should be noted that our findings can represent only an indication and not a discriminating criteria because our approach is based on several semiempirical assumptions. Among them the same scaling for the enthalpy and shear relaxation times has been assumed, but this possibility is not universally accepted. For example, in a recent paper, Echeverría and co-workers,³¹ compared enthalpy recovery, volume recovery and creep recovery experiments

in Se. In that work, creep and volume experiments resulted to be compatible with relaxation times having the same temperature dependence as viscosity whereas the enthalpy relaxation times showed a smoother temperature dependence. However it must be noted that these results were obtained by analyzing only the enthalpy relaxation isotherms with a phenomenological procedure, based on some empirical assumptions that could be criticizable. In fact, with a very similar analysis, different results³² have been recently obtained for the enthalpy and volume relaxation times which exhibited the same temperature dependence of the α relaxation times probed by dielectric and NMR spectroscopies in PVAc and PS, respectively. Malek also compared enthalpy and volume relaxation processes in glasses on the basis of the fictive relaxation rate R_f ³³ and evidenced a good agreement for many polymeric and nonpolymeric systems. The investigations of other researchers, however, showed significant differences in the equilibration times of different properties.^{34–36} As far as the subject of the present work is concerned, very interesting results were obtained by using the modulated calorimetry technique that allows one to investigate the enthalpy relaxation in the linear response regime above the glass transition. A close agreement among dielectric and enthalpy relaxation data was recently found in maltitol and sorbitol,³⁷ and in two different molecular weight polypropylene glycol samples.³⁸

Similarly, Jeong and Moon³⁹ found the same temperature dependence for shear relaxation times and enthalpy relaxation times in the low molecular weight glass former CKN.

V. Conclusions

This work deals with the possibility of describing the out-of-equilibrium DSC experiments in a low molecular weight PMMA sample, in the framework of a modified TNM approach.

The temperature dependence of the equilibrium fluctuations of the enthalpy below the glass transition is assumed to follow closely the extrapolated VFT behavior of the viscosity. This assumption is to some extent validated a priori by the low molecular weight of our sample. In fact, this rules out the effects due to the entanglement in high polymers, which results in different segmental and terminal relaxations. An important consequence of the above assumption should be the a posteriori checking of the consistency of the relaxations of these observables, offloading the inconsistencies observed in some literature works on to the TNM handling of the nonlinear effects of the out-of-equilibrium dynamics of glassy polymers.

The results of the present work indicate the possibility mentioned above, when the modified TNM approach is used. Moreover, as expected, our procedure provides a value of the prefactor of the enthalpic relaxation time of the same order of the atomic vibrations.

Furthermore, the analysis of two relaxational enthalpy isotherms obtained at different annealing temperatures suggests that the VFT parametrization of the segmental relaxation has to be preferred to the smoother temperature dependence predicted by the entropy-derived Avramov's model, both of them fairly well reproducing the PMMA viscosity above T_g . It is worthwhile to emphasize that this modified approach provided similar agreement with DSC experiments with respect

to the standard AGV model, so that the results of the present work do not represent a conclusive proof of the scaling behavior of the enthalpy and shear relaxation times.

References and Notes

- (1) Brawer, S. *Relaxation in Viscous Liquids and Glasses*; American Ceramic Society: Columbus, OH, 1983.
- (2) Angell, C. A.; Ngai, K. L.; McKenna, G. B.; McMillan, P. F.; Martin, S. W. *J. Appl. Phys.* **2000**, *88*, 3113.
- (3) Moynihan, C. T.; Lee, S. K.; Minami, T. *Thermochim. Acta* **1996**, *280/281*, 153.
- (4) Robinson, C. G.; Santangelo, P. G.; Roland, C. M. *J. Non-Cryst. Solids* **2000**, *275*, 153.
- (5) Wang, Li-Min; Velikov, V.; Angell, C. A. *J. Chem. Phys.* **2002**, *117*, 10184.
- (6) Hodge, I. M. *J. Res. Natl. Inst. Stand. Technol.* **1997**, *102*, 195.
- (7) Hutchinson, J. M.; Ruddy, M. *J. Polym. Sci., Polym. Phys. Ed.* **1988**, *26*, 2341.
- (8) Hodge, I. M. *Macromolecules*, **1987**, *20*, 2897.
- (9) Hutchinson, J. M.; Montserrat, S.; Calventus, Y.; Cortés, P. *Macromolecules* **2000**, *33*, 5252.
- (10) Andreozzi, L.; Faetti, M.; Giordano, M.; Palazzuoli, D. *Philos. Mag. B* **2002**, *82*, 397.
- (11) Tool, A. Q. *J. Am. Ceram. Soc.* **1946**, *29*, 240.
- (12) Hodge, I. M. *J. Non-Cryst. Solids* **1994**, *169*, 211.
- (13) Narayanaswamy, O. S. *J. Am. Ceram. Soc.* **1971**, *54*, 491.
- (14) Moynihan, C. T.; Easteal, A. J.; DeBolt, M. A.; Tucker, J. J. *Am. Ceram. Soc.* **1976**, *59*, 12.
- (15) Scherer, G. W. *J. Am. Ceram. Soc.* **1984**, *67*, 504.
- (16) Adam, G.; Gibbs, J. H. *J. Chem. Phys.* **1965**, *43*, 139.
- (17) Vogel, H. *Phys. Z.* **1921**, *22*, 645.
- (18) Fulcher, G. S. *J. Am. Ceram. Soc.* **1925**, *8*, 339.
- (19) Tammann, G.; Hesse, W. Z. *Anorg. Allg. Chem.* **1926**, *156*, 245.
- (20) Avramov, I.; Gutzov, I. *J. Non-Cryst. Solids* **2002**, *298*, 67.
- (21) Tverjanovich, A. *J. Non-Cryst. Solids* **2002**, *298*, 226.
- (22) Richardson, M. J.; Savill, N. G. *Polymer* **1975**, *16*, 753.
- (23) Ferry, J. D. *Viscoelastic Properties of Polymers*, 3rd ed.; Wiley: New York, 1980.
- (24) Avramov, I. *J. Non-Cryst. Solids* **2000**, *262*, 258.
- (25) Nedler, J. A.; Mead, R. *Comput. J.* **1965**, *7*, 308.
- (26) Andreozzi, L.; Faetti, M.; Giordano, M.; Palazzuoli, D. *J. Phys.: Condens. Matter* **2003**, *15*, S1215.
- (27) Cowie, J. M. G.; Ferguson, R. *Polymer* **1993**, *34*, 2135.
- (28) Andreozzi, L.; Faetti, M.; Giordano, M.; Palazzuoli, D. *J. Non-Cryst. Solids* **2003**, *332*, 229.
- (29) Di Marzio, E. A.; Yang, A. J. M. *J. Res. Natl. Inst. Stand. Technol.* **1997**, *102*, 135.
- (30) O'Connell, P. A.; McKenna, G. B. *J. Chem. Phys.* **1999**, *110*, 11054.
- (31) Echeverria, I.; Kolek, P. L.; Plazek, D. J.; Simon, S. L. *J. Non-Cryst. Solids* **2003**, *324*, 242.
- (32) Rault, J. *J. Phys.: Condens. Matter* **2003**, *15*, S1193.
- (33) Málek, J.; Montserrat, S. *Thermochim. Acta* **1998**, *313*, 191.
- (34) Cowie, J. M. G.; Harris, S.; McEwen, L. *J. Macromolecules* **1998**, *31*, 2611.
- (35) Cowie, J. M. G.; Ferguson, R.; Harris, S.; McEwen, L. *J. Polymer* **1998**, *39*, 4393.
- (36) McKenna, G. B.; Leterrier, Y.; Schultheisz, C. R. *Polym. Eng. Sci.* **1995**, *35*, 403.
- (37) Carpentier, L.; Descamps, M. *J. Phys. Chem. B* **2003**, *107*, 271.
- (38) Moon, I. K.; Jeong, Y. H.; Furukawa, T. *Thermochim. Acta* **2001**, *377*, 97.
- (39) Jeong, Y. H.; Moon, I. K. *Phys. Rev. B* **1995**, *52*, 6381.

MA049334P